Landscape Ecol
DOI 10.1007/s10980-017-0538-3

RESEARCH ARTICLE

Urbanization and air quality as major drivers of altered spatiotemporal patterns of heavy rainfall in China

Peijun Shi · Xuemei Bai · Feng Kong · Jiayi Fang · Daoyi Gong · Tao Zhou · Yan Guo · Yansui Liu · Wenjie Dong · Zhigang Wei · Chunyang He · Deyong Yu · Jing'ai Wang · Qian Ye · Rucong Yu · Deliang Chen

Received: 13 March 2017 / Accepted: 23 May 2017
© The Author(s) 2017. This article is an open access publication

Abstract

Context Land use/land cover change and other human activities contribute to the changing climate on regional and global scales, including the increasing occurrence of extreme-precipitation events, but the relative importance of these anthropogenic factors, as compared to climatic factors, remains unclear.

Objectives The main goal of this study was to determine the relative contributions of human-induced and climatic factors to the altered spatiotemporal patterns of heavy rainfall in China during the past several decades.

Methods We used daily precipitation data from 659 meteorological stations in China from 1951 to 2010, climatic factors, and anthropogenic data to identify possible causes of the observed spatiotemporal patterns of heavy rainfall in China in the past several decades, and quantify the relative contributions between climatic and human-induced factors.

P. Shi (✉) · X. Bai (✉) · J. Fang · D. Gong · T. Zhou · Y. Guo · Y. Liu · W. Dong · Z. Wei · C. He · D. Yu · J. Wang · Q. Ye
State Key Laboratory of Earth Surface Processes and Resource Ecology, Beijing Normal University, Beijing, China
e-mail: spj@bnu.edu.cn

X. Bai
e-mail: xuemei.bai@anu.edu.au

P. Shi
Key Laboratory of Environmental Change and Natural Disaster of Ministry of Education, Beijing Normal University, Beijing, China

P. Shi · F. Kong · J. Fang
Academy of Disaster Reduction and Emergency Management, Ministry of Civil Affairs & Ministry of Education, Beijing, China

X. Bai
Fennier School of Environment and Society, Australian National University, Canberra, Australia

F. Kong
China Meteorological Administration Training Center, Beijing, China

Y. Liu
College of Resources Science & Technology, Beijing Normal University, Beijing, China

J. Wang
Faculty of Geographical Sciences, Beijing Normal University, Beijing, China

R. Yu
China Meteorological Administration, Beijing, China

D. Chen
Department of Earth Sciences at the University of Gothenburg, Gothenburg, Sweden

Published online: 30 May 2017

Results Our analysis suggests that a total of 84.7–87.5% of the variance in heavy rainfall factors could be explained by large-scale climate phenomena and the local/regional anthropogenic activities. In particular, urbanization and air pollution together explained 58.5–65.5% of the variance. The spatial distribution of heavy rainfall amount and days over time shows a significant and increasing correlation with the spatial distributions of population density and annual low-visibility days.
Conclusions Our results suggest that the substantial increase in heavy rainfall across much of China during the past six decades is likely triggered by local and regional anthropogenic factors. Our results call for a better understanding of local and regional anthropogenic impacts on climate, and the exacerbated extreme climate events as a potential consequence of urbanization and air pollution.

Keywords Anthropogenic factors · Air pollution · Trigger · Heavy rainfall · China

Introduction

Both modeling results and observation data show an increase in the number of extreme precipitation events (Alexander et al. 2006; Beniston et al. 2007; Qian et al. 2007; Wang et al. 2008). This trend is typically explained by climate change, and is expected to exacerbate with the increase of greenhouse gas emissions (Easterling et al. 2000; Durman et al. 2001; Allen and Ingram 2002; Field et al. 2012; IPCC-AR5 2013). However, climate model simulations often underestimate the observed increase in heavy rainfall during the last five decades (Allen and Ingram 2002; Wilby and Wigley 2002; Min et al. 2011), which points to causes other than those traditionally considered in climate models, and the importance of considering anthropogenic factors (Allan and Soden 2008; Li et al. 2011). A recent research found that the climate models used by the IPCC AR5 capture reasonably the temporal trends of extreme precipitation during 1961–2000 in western China. However, the models do not adequately reproduce the trends over eastern China, which is characterized by much more intense anthropogenic activity (Shepherd 2005). Studies found that convective rainfall has experienced greater increase than stratiform precipitation: given that the former is influenced mostly by local interactions and the later by planetary circulation (Wang and Zhou 2005; Ou et al. 2013), the increased frequency of heavy rainfall events (Chen et al. 2010; Ou et al. 2013) might be due to human induced local changes. This highlights the need to explore more deeply the specific roles of a range of anthropogenic processes and their relative contributions to heavy rainfall at regional scales.

Data and methods

Data source

Precipitation data for 659 meteorological stations and annual haze days are from China Meteorological Administration; 29 large scale climate factors influencing China's precipitation are from NOAA and Chinese National Climate Center (Table 1); precipitable water and water vapor flux data of NCEP/NCAR and ERA/ECMWF reanalysis data; horizontal visibility data for 1957–2005 are from the Chinese Academy of Meteorological Sciences; and 11 country-level socio-economic and environmental indicators including GDP; primary, secondary and tertiary industrial output; construction-sector output; energy consumption; total population; urban population; rural population; urbanization ratio; annual average haze days; and county-level population density and horizontal visibility data are compiled from 60-year Statistics of New China and Prefectural (Municipal) Social and Economic Statistics Summary of China. Such 40 factors include 29 climatic factors and 11 anthropogenic factors. The former mainly covers regional circulation factors, the latter mainly refers to elements representing economic and social activities of human beings.

The heavy rainfall amounts, heavy rainfall days and heavy rainfall intensity of inter-annual and decadal heavy rain in China are calculated based on precipitation from 659 stations, configuration of which remains consistent through the research period. IDW (Inverse Distance Weight) interpolation method is used to produce spatially continuous raster layer of heavy rainfall factors.

Table 1 29 large scale climate factors and 11 socioeconomic factors

No.	Climate Factors	Description	Source
1	WPSH ANNUAL	West Pacific subtropical high, annual mean	NCC
2	WPSH SA	West Pacific subtropical high, seasonally averaged (JJA)	NCC
3	EASMI	The East Asian summer monsoon (EASM) index is defined as an area-averaged seasonally (JJA) dynamical normalized seasonality (DNS) at 850 hPa within the East Asian monsoon domain (10°N–40°N, 110°E–140°E)	CAS IAP LASG
4	SCSSMI	The South China Sea summer monsoon index (SCSSMI) is defined as an area-averaged seasonally (JJAS) dynamical normalized seasonality (DNS) at 925 hPa within the South China Sea monsoon domain (0°N–25°N, 100°E–125°E).	CAS IAP LASG
5	SASMI	The South Asian summer monsoon index (SASMI) is defined as an area-averaged seasonally (JJAS) dynamical normalized seasonality (DNS) at 850 hPa within the South Asian domain (5°N–22.5°N, 35°E–97.5°E)	CAS IAP LASG
6	SASMI1	Southwest Asian Summer Monsoon (SWASM) over the Southwest Asia (2.5°N–20°N, 35°E–70°E) June–September monthly mean	CAS IAP LASG
7	SASMI2	Southeast Asian Summer Monsoon (SEASM) over the Southeast Asia (2.5°N–20°N, 70°E–110°E), June- September monthly mean	CAS IAP LASG
8	ENSO DJF	El Niño-Southern oscillation, seasonally averaged (last year December–February, DJF)	NOAA CPC
9	ENSO MAM	Seasonally averaged (March–May, MAM)	NOAA CPC
10	ENSO JJA	Seasonally averaged (June–August, JJA)	NOAA CPC
11	ENSO SON	Seasonally averaged (September–Novermber, SON)	NOAA CPC
12	PDO	Standardized values for the PDO index, derived as the leading PC of monthly SST anomalies in the North Pacific Ocean. Annual mean	NOAA CPC
13	Pacific Warmpool	1st EOF of SST (60°E–170°E, 15°S–15°N) SST EOF, Annual mean	NOAA CPC
14	NINO3_4	East Central Tropical Pacific SST* (5°N–5°S) (170° –120°W), Annual mean	NOAA CPC
15	AMO US	Atlantic multidecadal oscillation index unsmoothed, annual mean	NOAA PSD
16	AMO SM	Atlantic multidecadal oscillation index smoothed, annual mean	NOAA PSD
17	Blocking	The blocking index is the frequency of DJF "blocked days" for Neutral, Warm and Cold episodes.	NOAA CPC
18	DMI MAM	Intensity of the IOD is represented by anomalous SST gradient between the western equatorial Indian Ocean (50°E–70°E and 10°S–10°N) and the south eastern equatorial Indian Ocean (90°E–110°E and 10°S–0°N). This gradient is named as Dipole Mode Index (DMI). Seasonally averaged (March–May, MAM)	JAMSTEC
19	DMI JJA	DMI seasonally averaged (June–August, JJA)	JAMSTEC
20	DMI SON	DMI seasonally averaged (September–Novermber, SON)	JAMSTEC
21	DMI DJF	DMI seasonally averaged (last year December–February, DJF)	JAMSTEC
22	DMI ANNUAL	DMI annual mean	JAMSTEC
23	TPH 1	Tibetan plateau high 25°N–35°N, 80°E–100°E annual mean	NCC
24	TPH 2	Tibetan plateau high 30°N–40°N, 75°E–105°E annual mean	NCC
25	QBO	Quasi-biennial oscillation annual mean	NOAA PSD
26	NHPVII	The northern hemisphere polar vortex intensity index, annual mean	NCC
27	AO	The monthly AO index (AOI) is defined as the difference in the normalized monthly zonal-mean sea level pressure (SLP) between 35°N and 65°N. Annual mean	CAS IAP LASG

Table 1 continued

No.	Climate Factors	Description	Source
28	AAO	The monthly AAO index (AAOI) is defined as the difference in the normalized monthly zonal-mean sea level pressure (SLP) between 40°S and 70°S. Annual mean	CAS IAP LASG
29	NAO	The NAO index (NAOI) is defined as the difference in the normalized monthly sea level pressure (SLP) regionally zonal-averaged over the North Atlantic sector from 80°W to 30°E between 35°N and 65°N. Annual mean	CAS IAP LASG
30	GDP	Gross domestic product	SNC-PSESS
31	GDP1	Agricultural production	SNC-PSESS
32	GDP2-1	Construction product	SNC-PSESS
33	GDP2	Industrial production	SNC-PSESS
34	GDP3	Service product	SNC-PSESS
35	TP	Total population	SNC-PSESS
36	RP	Rural population	SNC-PSESS
37	UP	Urban population	SNC-PSESS
38	UR	Urbanization Rate	SNC-PSESS
39	TEP	Total energy production	SNC-PSESS
40	HD	Annual mean haze day	SNC-PSESS

① No. 13 and No. 15 is from 1950 to 2008; No. 17 is from 1950 to 2000; No. 18–22 is from 1958 to 2010; Values out of time scale of 1951–2010 shall be replaced by average values. ② *NCC* National Climate Center, China, *CAS* Chinese Academy of Sciences, *IAP* Institute of Atmospheric Physics, *LASG* State Key Laboratory of Numerical Modeling for Atmospheric Sciences and Geophysical Fluid Dynamics in China, *NOAA* Oceanic and Atmospheric Administration, *NOAA CPC* NOAA Climate Prediction Center, *NOAA PSD* NOAA Physical Science Division, *JAMSTEC* Japan Agency for Marine-Earth Science and Technology. ② The second column WPSH ANNUAL, ENSO DJF, AMO US and AAO are selected as climate factors in the article. ③ *SNC-PSESS* 60-year Statistics of New China and Prefectural (Municipal) Social and Economic Statistics Summary of China

Methods

Calculation of heavy rainfall

In this research, heavy rainfall is defined as daily rainfall greater than 50 mm. The sum of HRA_i and heavy rainfall days HRD_i of each meteorological station as well as average heavy rainfall intensity HRI_i were calculated as per formulae (1)–(3), for the 6 decades of 1951–1960, 1961–1970, 1971–1980, 1981–1990, 1991–2000 and 2001–2010 respectively.

$$HRA_i = \sum_{j=1}^{10} hra_{1940+10i+j} \tag{1}$$

$$HRD_i = \sum_{j=1}^{10} hrd_{1940+10i+j} \tag{2}$$

$$HRI_i = \sum_{j=1}^{10} hra_{1940+10i+j} \Big/ \sum_{j=1}^{10} hrd_{1940+10i+j} \tag{3}$$

Notes wherein, HRA_i is total heavy rainfall amount at a meteorological station in the i th decade within a study phase; $hra_{1940+10i+j}$ total heavy rainfall amount at a meteorological station in the j th year of i th decade; HRD_i total heavy rainfall days at a meteorological station in the i th decade; $hrd_{1940+10i+j}$ total heavy rainfall days at a meteorological station in the j th year of i th decade; HRI_i heavy rainfall intensity at a meteorological station in the i th decade; i decadal order ($i = 1, 2, \ldots 6$); j yearly order ($j = 1, 2, \ldots 10$).

Model selection and validation

(1) Stepwise regression: Here we considered 40 factors (i.e. the 29 climate factors and 11 anthropogenic factors) as the candidate predictors and heavy rainfall (i.e. HRA, HRD, and HRI) as the target variables. Stationarity test and cointegration test are performed to eliminate the possibility of spurious regression. In

each selecting step, only those variables significant at the 95% level are identified and included in the regression equation. In the removing step, the variables not significant at the 90% level are ruled out from the equation (Johansen 1994).

(2) AIC to confirm model optimal variables: We use the Aakaike Information Criterion (AIC), as a criteria for model selection that penalize models having large number of predictors and search for the models that have small values of AIC (Cahill 2003).

(3) Cross-validation test the robustness and stability of the regression model: To address the issue of over-fit, we conducted cross-validation by intentionally leaving out up to 33% of data and used them to verify the model prediction.

MLR-based variance explanation rate

A MLR equation was established for standardized sequence based on the multiple regression theory (Harris 1992; Pedroni and Peter 1999; Mackinnon 2010):

$$Y_i = b_1X_{1i} + b_2X_{2i} + b_3X_{3i} + b_4X_{4i} + b_5X_{5i} + b_6X_{6i}$$

wherein, i = 1,…, n, n = 60 years and $b_1 \ldots b_6$ are regression coefficients.

wherein, r_1, r_2, r_3, r_4, r_5 and r_6 are correlation coefficient between heavy rain and WPSH, ENSO (HRA and HRD)/AMO (HRI), AAO, GDP2, UP and HD respectively. It was proved that:

$$c^2 = b_1r_1 + b_2r_2 + b_3r_3 + b_4r_4 + b_5r_5 + b_6r_6$$

wherein, c is multiple correlation coefficient, c^2 represents the six factors' rate of variance explanation of heavy rainfall and the $b_1r_1, b_2r_2, b_3r_3, b_4r_4, b_5r_5, b_6r_6$ represent respectively contributions of each factor to heavy rainfall in China.

Spatial correlation analysis

Spatial correlations are performed between county level raster images of HRA, HRD, HRI (which are generated using IDW) and population density (PD) and low visibility days (LVD). Higher spatial similarities between the two images compared would produce higher spatial correlation value. (Gao and Deng 2002).

Results

Trend in heavy rainfall in China

Since 1950s, the total precipitation amount for China shows no obvious trend, whereas both the intensity of heavy rainfall and the area suffering from extreme precipitation events have expanded (Zhai et al. 2005). HRA, HRD and HRI has increased significantly (Fig. 1): from the 1950s to the 2000s, HRA, HRD and HRI increased by 58.6–68.7, 46.5–60.2, and 7.1–11.5 percent respectively. Note that higher numbers are average of 659 station data, which tend to overestimate due to more stations in southeast China where most of the increase occurred; and the lower numbers are from the 0.5° grid data based on Ou et al. (2013), which tends to give lower estimation due to the smoothing effect of the interpolation. The share of heavy rainfall in total rainfall increased from 15.9% to 26.0% (Table 2). This increase demonstrates a clear, shifting spatial pattern with high values of HRA (Fig. 2; Table 3) and HRD (Fig. 3; Table 4) moving progressively from the southeast coast to inland China during the last 60 years. Such spatial–temporal features are obviously inconsistent with that of the warming temperature (Yatagai and Yasunari 1994; Shi et al. 2014) and cannot be reasonably explained by the leading atmospheric and oceanic climate factors (Easterling et al. 2000; Liu et al. 2009; Wan et al. 2012). Below we investigate, using climate and socioeconomic data, whether, and if so to what extent, local and regional anthropogenic processes contributed to the observed trend and pattern.

Temporal analysis: identifying key factors influencing heavy rainfall and their relative contributions

Factors influencing heavy rainfall

29 climate factors that are known to influence East Asian precipitation and 11 socioeconomic factors are considered as candidate predictors with heavy rainfall as the target variable (Table 1). Seven factors are

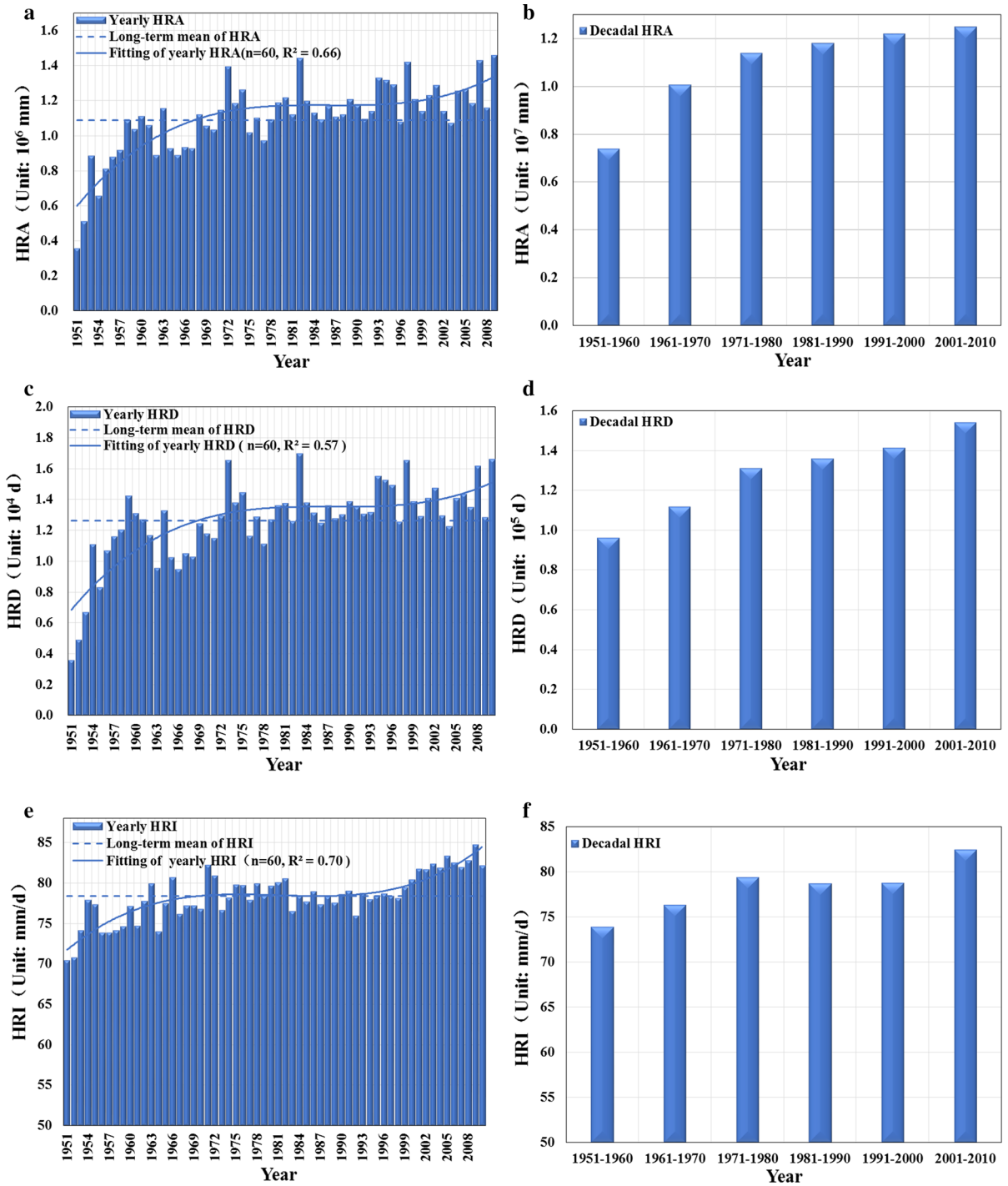

Fig. 1 Yearly and decadal heavy rainfall amounts, days and intensity in China from 1951 to 2010. **a** Yearly HRA in China. **b** Decadal HRA in China. **c** Yearly HRD in China. **d** Decadal HRD in China. **e** Yearly HRI in China. **f** Decadal HRI in China

eventually chosen as significantly related to heavy rainfall (0.05 significance level): four climatic factors including WPSH (western Pacific Subtropical High), ENSO (El Nino-Southern Oscillation), AMO (Atlantic Multi-decadal Oscillation) and AAO (Antarctic Oscillation), and 3 socio-economic factors including output

Table 2 The share of heavy rainfall in total rainfall in different decade in China

Decade	Heavy rainfall amounts (%)	Heavy rainfall day (%)
1951–1960	15.93	1.66
1961–1970	19.94	1.72
1971–1980	22.38	1.99
1981–1990	22.20	1.82
1991–2000	24.04	2.07
2001–2010	25.97	2.39

value of the secondary industry (GDP2), urban population (UP) and annual average haze days (HD). The four climatic factors are determined by large-scale climate dynamics and not directly influenced by local human activities. The three socio-economic factors are all closely related to land-use change and air pollution (Bai et al. 2012; Ding and Liu 2014), with urban population being an indirect demographical indicator of land-use change, GDP2 most indirect indicator for air pollution, and HD represents the environmental consequence of land-use change and air pollution, which is most closely linked to the air quality.

A Pearson correlation analysis shows that all three anthropogenic factors correlate very strongly with heavy rainfall (all significant at the 0.01 significance level), whereas the climate factors tend to be correlated less strongly and at statistically less significant levels (Table 5).

The influence of water vapor increment on heavy rainfall

Atmospheric precipitable water (PW) and divergence of water-vapour flux (WVF) can affect regional precipitation. We calculated regional total column PW and (surface—300 hPa) divergence of WVF in eastern and central China where significant increase in heavy rainfall occurred. As shown in Fig. 4, PW and divergence of the WVF increase until the end of 1980s but decline afterwards, none of which converge with the trend in heavy rainfall. The spatial distributions of the changes in the two variables between 1970 and 2010 indicate that both PW and WVF decreased in most of the areas where heavy rainfall actually increased. In addition, during the last two decades the proportion of decadal convective HRD to total HRD increased from 81.8 to 86.0%, with a corresponding drop in the proportion of continuous HRD to total HRD, suggesting that the increase in heavy rainfall is increasingly influenced by local conditions rather than the large-scale circulation and moisture fluxes.

Quantifying relative contributions

To estimate the relative contributions of these seven factors to the observed increase in heavy rainfall, we performed multiple linear regression. The selected factors collectively explained 85.8, 84.7 and 87.5% of the total variance of HRA, HRD and HRI respectively. Anthropogenic factors are the main contributors, each contributing at equivalent magnitude and collectively accounting for 71.7, 69.0 and 75.0% of the total explained variance whereas the climate factors account for only 28.3, 31.0 and 25.1% (Table 5). Each of the three anthropogenic factors has roughly the same level of contribution as the sum of all the climate factors. Combined together, they are thrice as likely to have led to the variance in heavy rainfall than the climate factors.

Table 3 Change of station number of decadal HRA in China from 1951 to 2010

Year	HRA grade (unit: mm)				
	<1000	1000–2000	2000–3000	3000–4000	>4000
1951–1960	405 (61.46%)	111 (16.84%)	82 (12.44%)	25 (3.79%)	36 (5.46%)
1961–1970	336 (50.99%)	93 (14.11%)	106 (16.08%)	62 (9.41%)	62 (9.41%)
1971–1980	340 (51.59%)	116 (17.60%)	91 (13.81%)	54 (8.19%)	58 (8.80%)
1981–1990	342 (51.90%)	99 (15.02%)	95 (14.42%)	61 (9.26%)	62 (9.41%)
1991–2000	358 (54.32%)	89 (13.51%)	78 (11.84%)	56 (8.50%)	78 (11.84%)
2001–2010	359 (54.48%)	64 (9.71%)	83 (12.59%)	50 (7.59%)	103 (15.63%)

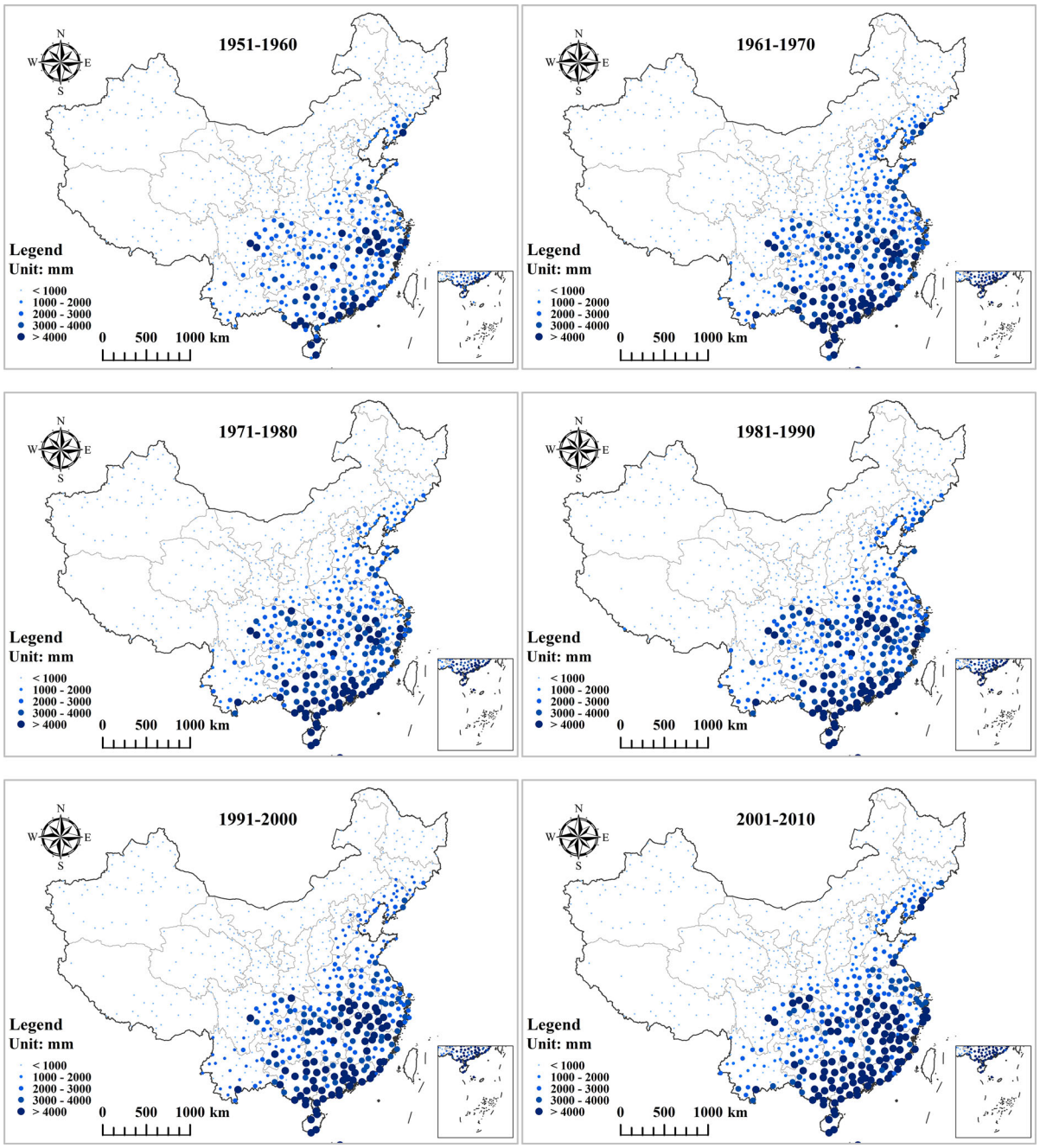

Fig. 2 Spatial distribution pattern of decadal HRA in China from 1951 to 2010

Robustness of the results

The robustness of our statistical model is tested through four different analyses. First of all, to evaluate the influence of various lag effects of the alternative factors that are not included in our model, we have performed power spectrum analysis to obtain the possible lag time of all the input variables, and conducted an un-interpreted residual analysis. Results show that the variance explained percentage of HRA, HRD and HRI are 6.9, 6.3 and 5.3% respectively (Table 6), which are very small

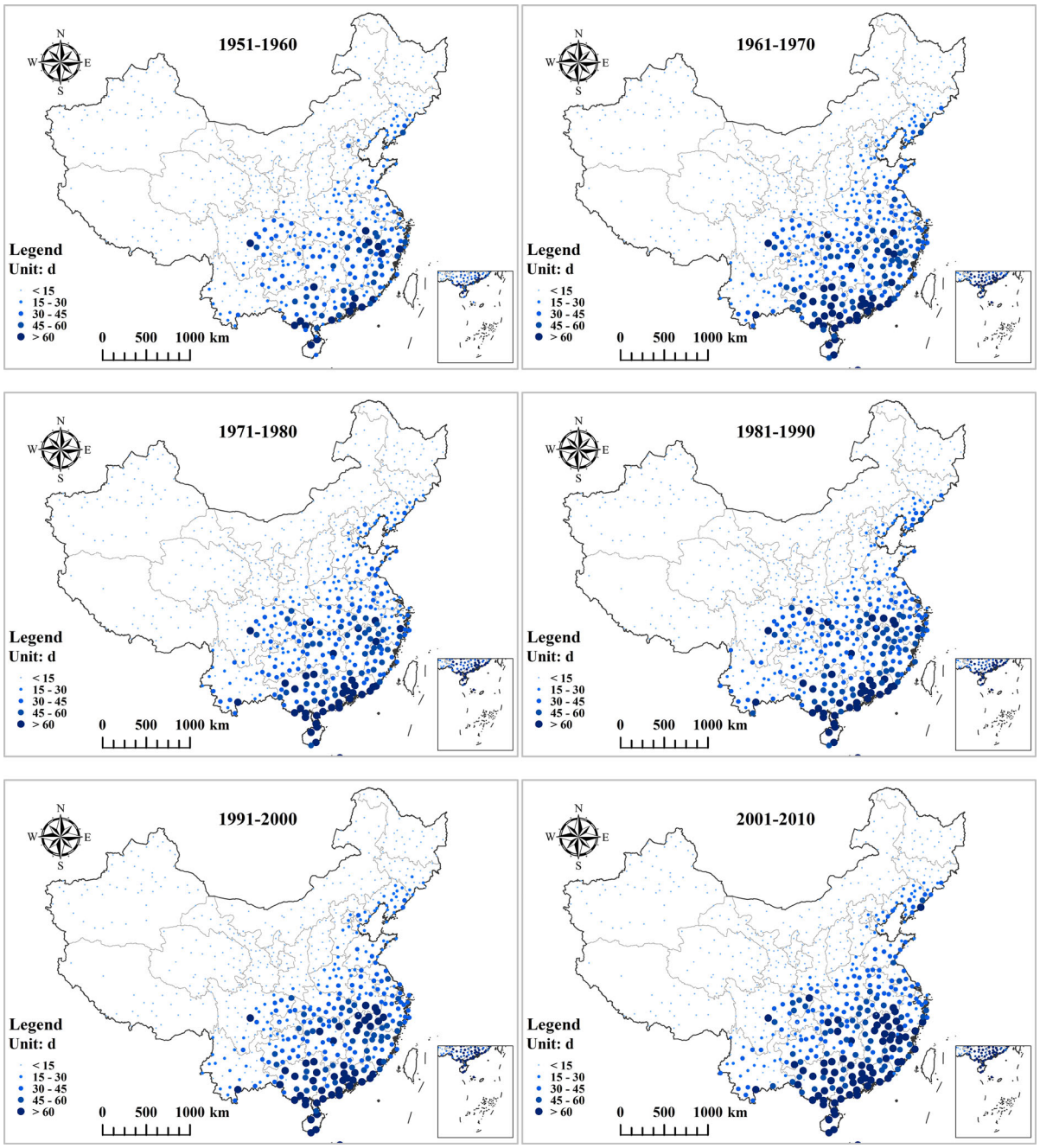

Fig. 3 Spatial distribution pattern of decadal HRD in China from 1951 to 2010

compared to the explained variance percentage of our model. This means the factors included in our model through step-wise regression is robust, despite the limitation of the method. In addition, using a different heavy rainfall threshold (95 percentile) gave consistent results. Furthermore, we also used the Akaike Information Criterion (AIC) as a criteria for model selection that penalize models having large number of predictors (Table 7), and finally a cross-validation analysis leaving out up to 33% of

Table 4 Change of station number of decadal HRA in China from 1951 to 2010

Year	HRD grade (unit: day)				
	<1000	1000–2000	2000–3000	3000–4000	>4000
1951–1960	418 (63.43%)	130 (19.73%)	63 (9.56%)	28 (4.25%)	20 (3.03%)
1961–1970	349 (52.96%)	117 (17.75%)	102 (15.48%)	52 (7.89%)	39 (5.92%)
1971–1980	346 (52.50%)	137 (20.79%)	93 (14.11%)	44 (6.68%)	39 (5.92%)
1981–1990	352 (53.41%)	111 (16.84%)	99 (15.02%)	54 (8.19%)	43 (6.53%)
1991–2000	366 (55.54%)	101 (15.33%)	96 (14.57%)	43 (6.53%)	53 (8.04%)
2001–2010	365 (55.39%)	70 (10.62%)	97 (14.72%)	53 (8.04%)	74 (11.23%)

Table 5 Correlation coefficient and variance explained percentage of climate and anthropogenic factors

Heavy rainfall and influencing factors		WPSH	ENSO	AMO	AAO	GDP2	UP	HD	CI	AI	Total
HRA	r	0.49**	–	−0.45*	0.72**	0.71**	0.79**	0.75**	0.51**	0.78**	0.78**
	VER	7.4%	–	7.3%	9.6%	17.9%	17.8%	25.9%	24.3%	61.5%	85.8%
HRD	r	0.49**	–	−0.44*	0.64**	0.67**	0.64**	0.70**	0.51**	0.71**	0.73**
	VER	8.8%	–	6.2%	11.2%	16.6%	18.9%	23.0%	26.2%	58.5%	84.7%
HRI	r	0.41*	0.39*	–	0.56**	0.72**	0.81**	0.84**	0.47*	0.84**	0.86**
	VER	6.5%	5.3%	–	10.1%	18.9%	20.0%	26.6%	21.9%	65.5%	87.5%

VER variance explained percentage, *r* correlation coefficient, *CI* climatic factors, *AI* anthropogenic factors

* Means correlation is significant at the 0.05 level, and ** at the 0.01 level

data (Table 8). Both results show high-level stability and robustness of our model.

To further illustrate the relative importance of the climatic and anthropogenic factors in increasing heavy rainfall, we produced normalized HRA, HRD and HRI. We also generated four integrated factors—integrated heavy rainfall index, integrated climatic indicator, integrated anthropogenic indicator and integrated natural-anthropogenic indicator—by normalizing the individual factors and integrating them using the variance explanation rate of the factor as respective weight, and plotted the scatter diagrams of these factors against normalized heavy rainfall factors (Fig. 5). In all cases, the integrated anthropogenic- and anthropogenic-climatic factor factors demonstrate much more synchronized trends with normalized and integrated heavy rainfall factors, with *R-square* of the fitting curves typically around 0.90. In contrast, the *R-square* of the fitting curves for the climatic factors are typically around 0.40. These findings reinforce that integrated anthropogenic factors explain much more the documented increase in heavy rainfall in China.

Spatial correlation between anthropogenic factors and heavy rainfall

If the anthropogenic processes indeed contributed more to the increasing trend in heavy rainfall, then the changing spatial pattern of anthropogenic processes should be related to the shifting spatial pattern of the heavy rainfall factors. We tested this via spatial correlation analysis between county level socioeconomic data and heavy rainfall indicators. Due to the limited data availability at this fine resolution over the long term, we used county-level population density (PD) to represent the spatial distribution of urbanization, and the annual average days with visibility less than 10 km (LVD) as a proxy indicator of HD, given that LVD can be affected by air pollution, and there is a statistically significant, high correlation between HD and LVD ($r = 0.79$, $p < 0.01$). The meteorological station data were interpolated to generate 1-km resolution images, based on which prefecture level mean values were generated. Figure 6 shows there are statistically significant high correlations between the county level heavy rainfall data and the urbanization

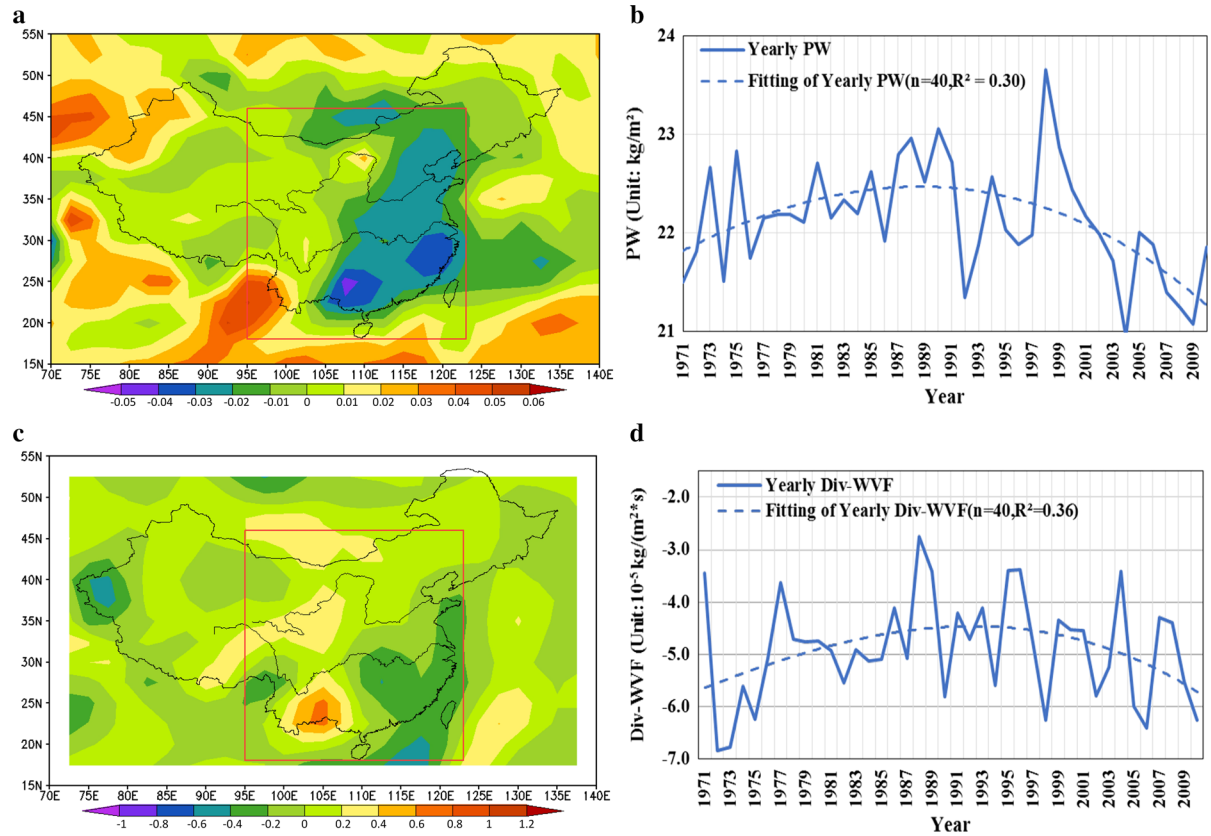

Fig. 4 Atmospheric precipitable water vapor and divergence of the water-vapour flux (Div-WVF) (surface—300 hPa) in the Central and East China: **a** Spatial distribution of changes in annual mean precipitable water vapour from NCEP/NCAR between 1971 and 2010 [kg/(m^{2}a)]; **b** Annual mean precipitable water (PW) vapour in central and east China (*red rectangular area* in Fig. 2a) from 1971 to 2010; **c** Spatial distribution of changes in annual mean divergence of the water-vapour flux from NCEP/NCAR between 1971–2010 [kg/(msa)]; **d** Annual mean divergence of the water-vapour flux in central and east China (*red rectangular area* in Fig. 2c) from 1971 to 2010

and air pollution over time and across space, with *r* steadily increasing over time (Table 9). Urbanization in China was rather stable until late 1970s and then accelerated in terms of scale and magnitude during the last three decades (Bai et al. 2014), coinciding with the increase of *r* and thus further supporting that land-use change resulting from urbanization and associated air pollution has indeed played a major role in the increase of heavy rainfall. Our tests show this result is not affected by potential spatial autocorrelation of variables.

Conclusion

All the results of our analyses point to the same conclusion: the decadal increases in, and shifting spatio-temporal patterns of, heavy rainfall in China during 1951–2010 are likely caused primarily by large scale and rapid urbanization and industrialization. A likely explanation is the climate impacts of land-use change triggered by urbanization: indeed, land–atmosphere interactions are known to affect both temperature (Seneviratne et al. 2006; Sun et al. 2014) and precipitation (Lowry 1998; Thielen et al. 2000; Li et al. 2011; Kaufmann et al. 2007). China has been urbanizing rapidly over the last three decades (Bai et al. 2014), driven by economic growth (Lambin and Patrick 2011; Bai et al. 2012). Urban land-use typically means more paved area, less vegetation and tall buildings, which can cause more convective rainstorms (Wan et al. 2012; Han et al. 2014; Jin et al. 2015). Moreover, industrialization is concurrent with urbanization in China, with most of the secondary

Table 6 Variance explained percentage of the different lag climate and anthropogenic factors related to the residual of HRA, HRD, HRI

Heavy rainfall and influencing factors		WPSH annual	WPSH SA	EASMI	ENSO DJF	ENSO MAM	AMO US	AAO	NAO	UP	GDP2	HD	CI	AI	Total
HRA	Lag	Lag 1	Lag 1	–	Lag 3	–	Lag 3	Lag 2	Lag 1	Lag 1	Lag 1	Lag 5	–	–	–
	VER	0.83%	0.31%	–	0.75%	–	0.67%	0.92%	0.41%	0.97%	0.89%	1.12%	3.89%	2.98%	6.87%
HRD	Lag	Lag 1	Lag 2	–	Lag 3	–	Lag 3	Lag 2	Lag 1	Lag 1	Lag 1	Lag 5	–	–	–
	VER	0.72%	0.36%	–	0.61%	–	0.53%	0.85%	0.37%	0.93%	0.91%	0.97%	3.44%	2.81%	6.25%
HRI	Lag	Lag 1	Lag 1	Lag 1	Lag 3	Lag 1	–	Lag 2	Lag 1	Lag 1	Lag 1	Lag 1	–	–	–
	VER	0.63%	0.33%	0.24%	0.43%	0.26%	–	0.41%	0.37%	0.81%	0.88%	0.90%	2.67%	2.59%	5.26%

VER variance explained percentage, *lag* indicator selected with different lag year, *CI* climatic factors, *AI* anthropogenic factors

Table 7 Akaike information criterion (AIC) of MLR

Dependent variable	Independent variables	Order number	AIC	Dependent variable	Independent variables	Order number	AIC	Dependent variable	Independent variables	Order number	AIC
HRA	UP	1	198.9	HRD	HD	1	190.7	HRI	HD	1	196.5
HRA	UP, HD	2	189.2	HRD	HD, GDP2	2	166.5	HRI	HD, UP	2	173.6
HRA	UP, HD, AAO	3	98.4	HRD	HD, GDP2, AAO	3	152.3	HRI	HD, UP, GDP2	3	165.4
HRA	UP, HD, AAO GDP2	4	165.6	HRD	HD, GDP2, AAO, UP	4	170.2	HRI	HD, UP, GDP2 AAO	4	179.1
HRA	UP, HD, AAO GDP2,WPSH	5	84.6	HRD	HD, GDP2, AAO UP, WPSH	5	112.5	HRI	HD, UP, GDP2 AAO, WPSH	5	121.5
HRA	UP, HD, AAO GDP2, WPSH, AMO	6	81.2	HRD	HD, GDP2, AAO UP, WPSH, AMO	6	96.3	HRI	HD, UP, GDP2 AAO, WPSH, ENSO	6	91.8

Table 8 Cross validation correlation coefficient of regression

Heavy rainfall	Leave-one-out cross validation	Leave-5-out cross validation	Leave-10-out cross validation	Leave-20-out cross validation
HRA	0.89**	0.88**	0.86**	0.85**
HRD	0.89**	0.88**	0.86**	0.85**
HRI	0.97**	0.95**	0.93**	0.91**

** Means correlation is significant at the 0.01 level

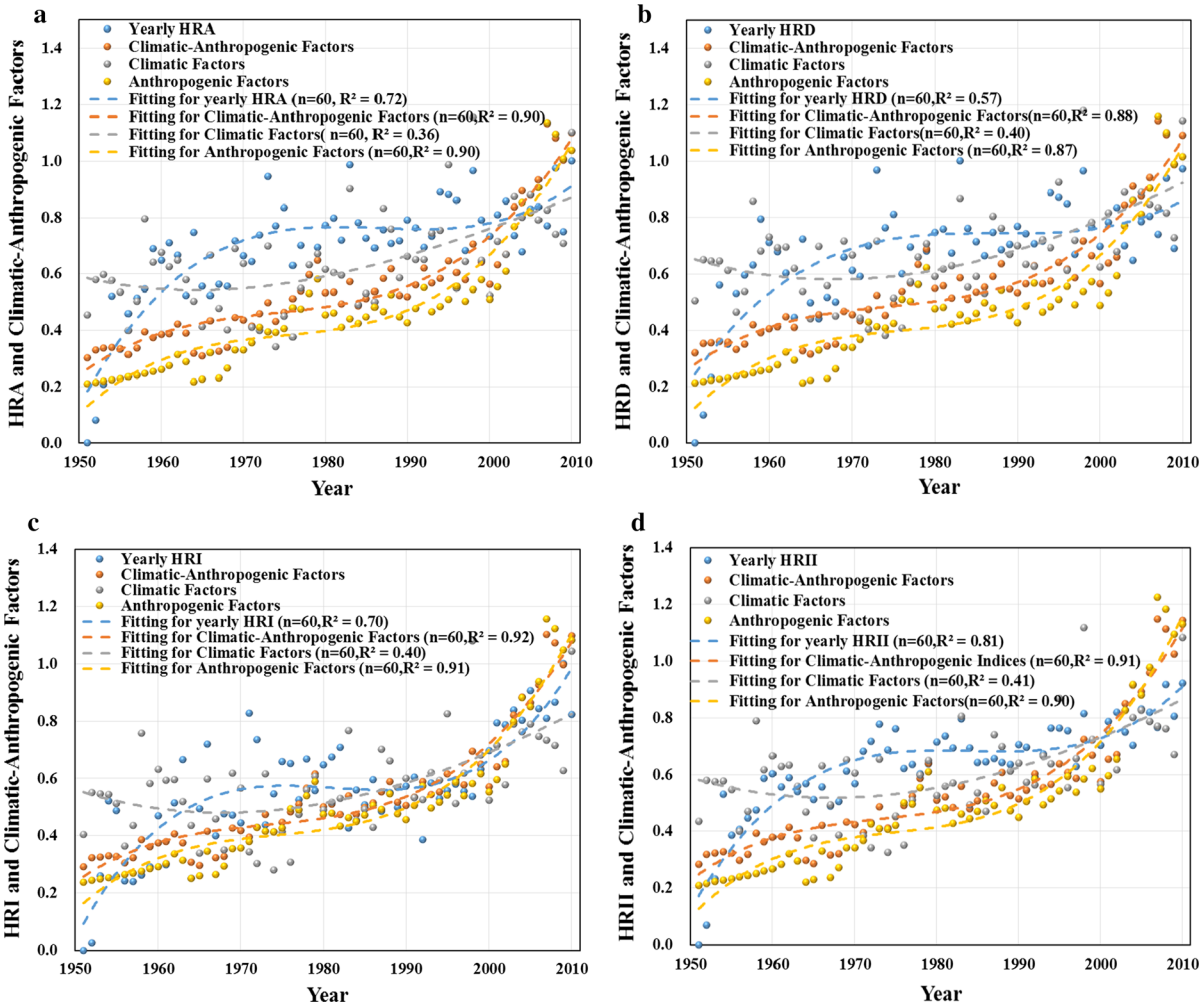

Fig. 5 Correlation between integrated climatic and anthropogenic factors and normalized heavy rainfall factors over Time. **a** Normalized HRA. **b** Normalized HRD. **c** Normalized HRI. **d** Integrated and normalized heavy rainfall index

industrial activities concentrated in cities and towns. Emissions resulting from industrial activities, the demand for heating and the rapidly growing use of personal cars in cities trigger a significant increase in hazy days (Ding and Liu 2014), which in turn suppresses the light rainfall and may enhance the strong convective rainstorms (Mölders and Olson 2004; Li et al. 2011).

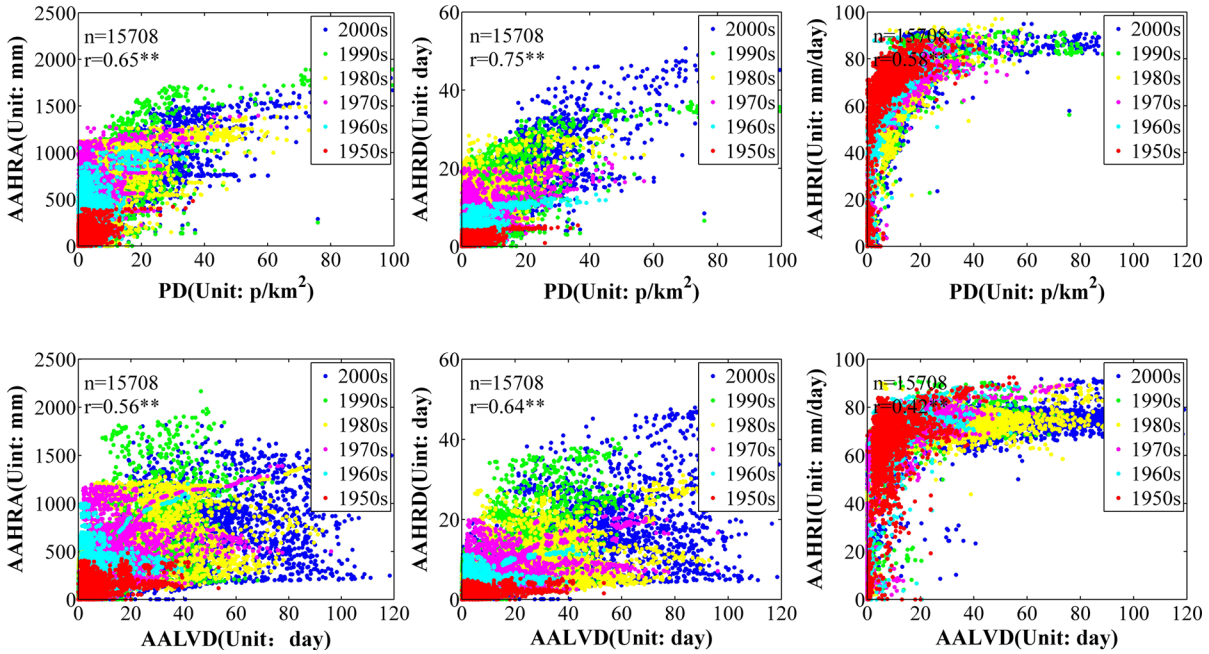

Fig. 6 Spatio-temporal correlation between county level annual average heavy rainfall (AAHRA, AAHRD, AAHRI) and population density (PD) and annual average low visibility days (AALVD). Data include 6 time sections for 2618 counties. Population density data are for 1953, 1964, 1982, 1990, 2000 and 2010; decadal horizontal visibility data are derived from data during 1957–2005; *asterisk* means correlation is significant at the 0.01 level

Table 9 Spatial correlation coefficient between county level heavy rainfall and PD & LVD

Heavy rainfall		Decade					
		1951–1960	1961–1970	1971–1980	1981–1990	1991–2000	2001–2010
HRA	PD	0.35**	0.36**	0.38**	0.42**	0.43**	0.45**
	LVD	0.35**	0.37**	0.41**	0.46**	0.49**	0.51**
HRD	PD	0.36**	0.37**	0.40**	0.46**	0.47**	0.50**
	LVD	0.36**	0.40**	0.43**	0.48**	0.51**	0.53**
HRI	PD	0.39**	0.41**	0.41**	0.48**	0.50**	0.51**
	LVD	0.48**	0.49**	0.57**	0.57**	0.58**	0.60**

n = 2618; ** Means correlation is significant at the 0.01 level

Previous studies linking urbanization to rainfall are mostly focusing on the impact on total rainfall and mostly considered only the local or city scale (Rosenfeld 2000; Ramanathan et al. 2001; Kaufmann et al. 2007; Alexander et al. 2013). Kishtawal et al. (2010) found urbanization as likely cause of increased heavy rainfall in India over five decades. Our results support this finding, but also show that urbanization is only one of the factors- air pollution contributes at equivalent magnitude. Our analysis is the first, to our knowledge, to statistically establish urbanization and air pollution as likely the primary cause of a nation- or sub-continental-scale increase in heavy rainfall over decades, and to quantify relative contributions of anthropogenic and climate factors.

Our findings indicate that local anthropogenic processes may shift the regional climate through mechanisms other than GHG emissions. The physical mechanism of such statistically robust connection needs to be better understood, and socio-economic and human dimensions need to be better reflected into the climate models. With cities in China increasingly

experiencing extreme rainfall events (Li et al. 2012), compounded by the increasing extreme summer heat in the same region (Sun et al. 2014), our findings call for a careful reevaluation of the risks of extreme weather in formulating national policies on urbanization, industrialization and environmental management, in China and elsewhere. Rapidly growing and industrializing cities and nations will need to better control the air pollution, and to anticipate and accommodate these regional climate consequences, if they are to reduce the risk of flooding and waterlogging.

Acknowledgements This research was supported by the 973 Project *"National Key Research and Development Program–Global Change and Mitigation Project: Global change risk of population and economic system: mechanisms and assessments"* under Grant No. 201531480029, Ministry of Science and Technology of China, People's Republic of China, the National Natural Science Foundation of Innovative Research Group Project "Earth Surface Process Model and Simulation" under Grant No. 41621061. We thank Ninad Bondre for his helpful comments and edits. We thank anonymous reviewers for their helpful comments. The analysis was undertaken in MATLAB and plots drawn in EXCEL, MATLAB and ArcGIS.

Open Access This article is distributed under the terms of the Creative Commons Attribution 4.0 International License (http://creativecommons.org/licenses/by/4.0/), which permits unrestricted use, distribution, and reproduction in any medium, provided you give appropriate credit to the original author(s) and the source, provide a link to the Creative Commons license, and indicate if changes were made.

References

Alexander LV, Allen SK, Bindoff NL, Bréon FM, Church JA, Cubasch U, Emori S, Forster P, Friedlingstein P, Gillett N (2013) Climate change 2013: the physical science basis. contribution of working group I to the fifth assessment report of the intergovernmental panel on climate change. Contrib Work 43(22):143–151

Alexander LV, Zhang X, Peterson TC, Caesar J, Gleason B, Tank A, Haylock M, Collins D, Trewin B, Rahimzadeh F, Tagipour A, Kumar KR, Revadekar J, Griffiths G, Vincent L, Stephenson DB, Burn J, Aguilar E, Brunet M, Taylor M, New M, Zhai P, Rusticucci M, Vazquez-Aguirre JL (2006) Global observed changes in daily climate extremes of temperature and precipitation. J Geophys Res Atmos 111:D5

Allan RP, Soden BJ (2008) Atmospheric warming and the amplification of precipitation extremes. Science 321(5895):1481–1484

Allen MR, Ingram WJ (2002) Constraints on future changes in climate and the hydrologic cycle. Nature 419(6903):224–232

Bai X, Chen J, Shi P (2012) Landscape urbanization and economic growth in China: positive feedbacks and sustainability dilemmas. Environ Sci Technol 46(1):132–139

Bai X, Shi P, Liu Y (2014) Realizing China's urban dream. Nature 509(7499):158–160

Beniston M, Stephenson DB, Christensen OB, Ferro CAT, Frei C, Goyette S, Halsnaes K, Holt T, Jylha K, Koffi B, Palutikof J, Schoell R, Semmler T, Woth K (2007) Future extreme events in European climate: an exploration of regional climate model projections. Clim Chang 81:71–95

Cahill AT (2003) Significance of AIC differences for precipitation intensity distributions. Adv Water Resour 26(4):457–464

Chen D, Ou T, Gong L, Xu C-Y, Li W, Ho C-H, Qian W (2010) Spatial interpolation of daily precipitation in China: 1951–2005. Adv Atmos Sci 27(6):1221–1232

Ding Y, Liu Y (2014) Analysis of long-term variations of fog and haze in China in recent 50 years and their relations with atmospheric humidity. Sci China Earth Sci 57(1):36–46

Durman CF, Gregory JM, Hassell DC, Jones RG, Murphy JM (2001) A comparison of extreme European daily precipitation simulated by a global and a regional climate model for present and future climates. Q J R Meteorol Soc 127(573):1005–1015

Easterling DR, Evans JL, Groisman PY, Karl TR, Kunkel KE, Ambenje P (2000) Observed variability and trends in extreme climate events: a brief review. Bull Am Meteorol Soc 81(3):417–425

Field C, Barros V, Stocker T, Dahe Q, Dokken D (2012) Special report: managing the risks of extreme events and disasters to advance climate change adaptation (SREX). Cambridge University Press, Cambridge

Gao ZQ, Deng XZ (2002) Analysis on spatial features of LUCC based on remote sensing and GIS in China. Chin Geogr Sci 12(2):107–113

Han J-Y, Baik J-J, Lee H (2014) Urban impacts on precipitation. Asia-Pac J Atmos Sci 50(1):17–30

Harris RID (1992) Testing for unit roots using the augmented Dickey-Fuller test: some issues relating to the size, power and the lag structure of the test. Econ Lett 38(4):381–386

IPCC-AR5 (2013) Climate change 2013: the physical science basis. IPCC. In: Working group I contribution to the fifth assessment report of the intergovernmental panel on climate change

Jin MS, Li Y, Su D (2015) Urban-induced mechanisms for an extreme rainfall event in Beijing China: a satellite perspective. Climate 3(1):193–209

Johansen SR (1994) The role of the constant and linear terms in cointegration analysis of nonstationary variables. Econom Rev 13(2):205–229

Kaufmann RK, Seto KC, Schneider A, Liu Z, Zhou L, Wang W (2007) Climate response to rapid urban growth: evidence of a human-induced precipitation deficit. J Clim 20(10):2299–2306

Kishtawal CM, Niyogi D, Tewari M, Pielke RA, Shepherd JM (2010) Urbanization signature in the observed heavy

rainfall climatology over India. Int J Climatol 30(13):1908–1916
Lambin EF, Patrick M (2011) Global land use change, economic globalization, and the looming land scarcity. Proc Natl Acad Sci 108(9):3465–3472
Li Z, Niu F, Fan J, Liu Y, Rosenfeld D, Ding Y (2011) Long-term impacts of aerosols on the vertical development of clouds and precipitation. Nat Geosci 4(12):888–894
Li K, Wu S, Dai E, Xu Z (2012) Flood loss analysis and quantitative risk assessment in China. Nat Hazards 63(2):737–760
Liu SC, Fu C, Chein-Jung S, Chen JP, Wu F (2009) Temperature dependence of global precipitation extremes. Geophys Res Lett 36(17):367–389
Lowry WP (1998) Urban effects on precipitation amount. Prog Phys Geogr 22(4):477–520
Mackinnon J (2010) Critical values for cointegration tests. Work Pap 5(1):107–122
Min S-K, Zhang X, Zwiers FW, Hegerl GC (2011) Human contribution to more-intense precipitation extremes. Nature 470(7334):378–381
Mölders N, Olson MA (2004) Impact of urban effects on precipitation in high latitudes. J Hydrometeorol 5(3):409–429
Ou T, Chen D, Linderholm HW, Jeong J-H (2013) Evaluation of global climate models in simulating extreme precipitation in China. Tellus A 65:1–16
Pedroni, Peter (1999) Critical values for cointegration tests in heterogeneous panels with multiple regressors. Oxf Bull Econ Stat 61(S1): 653–670(618)
Qian W, Fu J, Yan Z (2007) Decrease of light rain events in summer associated with a warming environment in China during 1961–2005. Geophys Res Lett 34(11):224–238
Ramanathan V, Crutzen P, Kiehl J, Rosenfeld D (2001) Aerosols, climate, and the hydrological cycle. Science 294(5549):2119–2124
Rosenfeld D (2000) Suppression of rain and snow by urban and industrial air pollution. Science 287(5459):1793–1796
Seneviratne SI, Lüthi D, Litschi M, Schär C (2006) Land–atmosphere coupling and climate change in Europe. Nature 443(7108):205–209
Shepherd JM (2005) A review of current investigations of urban-induced rainfall and recommendations for the future. Earth Interact 9(12):1–27
Shi P, Sun S, Wang M, Li N, Jin Y, Gu X, Yin W (2014) Climate change regionalization in China (1961–2010). Sci China Earth Sci 57(11):2676–2689
Sun Y, Zhang X, Zwiers FW, Song L, Wan H, Hu T, Yin H, Ren G (2014) Rapid increase in the risk of extreme summer heat in Eastern China. Nat Clim Chang 4:1082–1085
Thielen J, Wobrock W, Gadian A, Mestayer P, Creutin J-D (2000) The possible influence of urban surfaces on rainfall development: a sensitivity study in 2D in the meso-γ-scale. Atmos Res 54(1):15–39
Wan H, Zhong Z, Yang X, Li X (2012) Ensembles to model the impact of urbanization for a summertime rainstorm process in Yangtze River Delta, China. Meteorol Appl 22:105–112
Wang W, Chen X, Shi P, van Gelder PHAJM (2008) Detecting changes in extreme precipitation and extreme streamflow in the Dongjiang River Basin in southern China. Hydrol Earth Syst Sci Discuss 12(1):207–221
Wang Y, Zhou L (2005) Observed trends in extreme precipitation events in China during 1961–2001 and the associated changes in large-scale circulation. Geophys Res Lett 32(9):297–314
Wilby RL, Wigley TML (2002) Future changes in the distribution of daily precipitation totals across North America. Geophys Res Lett 29(7):39-31–39-34
Yatagai A, Yasunari T (1994) Trends and decadal-scale fluctuations of surface air temperature and precipitation over China and Mongolia during the recent 40 year period (1951–1990). J Meteorol Soc Jpn 72(6):937–957
Zhai PM, Zhang XB, Wan H, Pan XH (2005) Trends in total precipitation and frequency of daily precipitation extremes over China. J Clim 18(7):1096–1108